Clearly, at normal incidence, the resonant frequency of this mode must remain unchanged, as must the frequency at which the diffracted order begins to propagate. In the rotated geometry ($\varphi = 90°$), diffraction due to the rods will be in a plane orthogonal to the plane of incidence, and the frequency associated with the onset of diffraction will increase hyperbolically with wave vector ($k_y = k_0 \sin \theta$). Our measurements and modeling show (Fig. 5B) that close to normal incidence, the dispersion of the mode exhibits the expected dependence. The mode asymptotically approaches a frequency $\sim\nu_{cutoff}$ for larger values of k_y. A small difference between ν_{cutoff} and the observed limit is not surprising, as Eq. 1 does not take into account the finite length of the tubes. The results from the wax-filled sample thus fully confirm the expected behavior.

The idea of "designer" surface modes proposed by Pendry *et al.* (*6*) promises the ability to engineer a SP at almost any frequency. Our results verify the propagation of SP-like modes on structured, near perfectly conducting substrates. These new "metamaterials" offer the ability of applying near-field, surface plasmon–induced concepts, which have been well studied in the visible regime, to the microwave domain.

References and Notes

1. H. M. Barlow, A. L. Cullen, *Proc. IEE* **10**, 329 (1953).
2. R. Collin, *Field Theory of Guided Waves* (Wiley, New York, ed. 2, 1990), chap. 7.
3. R. H. Ritchie, *Phys. Rev.* **106**, 874 (1957).
4. H. Raether, *Surface Plasmons* (Springer-Verlag, Berlin, 1988), chap. 2.
5. W. L. Barnes, A. Dereux, T. W. Ebbesen, *Nature* **424**, 824 (2003).
6. J. B. Pendry, L. Martín-Moreno, F. J. García-Vidal, *Science* **305**, 847 (2004); published online 8 July 2004 (10.1126/science.1098999).
7. FEM computer modeling was done with the use of HFSS (Ansoft Corporation, Pittsburgh, PA).
8. A. P. Hibbins, J. R. Sambles, C. R. Lawrence, *J. Appl. Phys.* **87**, 2677 (2000).

22 December 2004; accepted 8 March 2005
10.1126/science.1109043

All-Optical Switching in Rubidium Vapor

Andrew M. C. Dawes, Lucas Illing, Susan M. Clark, Daniel J. Gauthier*

We report on an all-optical switch that operates at low light levels. It consists of laser beams counterpropagating through a warm rubidium vapor that induce an off-axis optical pattern. A switching laser beam causes this pattern to rotate even when the power in the switching beam is much lower than the power in the pattern. The observed switching energy density is very low, suggesting that the switch might operate at the single-photon level with system optimization. This approach opens the possibility of realizing a single-photon switch for quantum information networks and for improving transparent optical telecommunication networks.

An important component of high-speed optical communication networks is an all-optical switch, where an incoming "switching" beam redirects other beams through light-by-light scattering in a nonlinear optical material (*1*, *2*). For quantum information networks, it is important to develop optical switches that are actuated by a single photon (*3*). Unfortunately, because the nonlinear optical interaction strength of most materials is so small, achieving single-photon switching is difficult. This problem appears to be solved through modern quantum-interference methods, in which the nonlinear interaction strength can be increased by many orders of magnitude (*3*–*10*). It is also important to develop all-optical switches where the output beam is controlled by a weaker switching beam, so they can be used as cascaded classical or quantum computational elements (*11*). Current switches, in contrast, tend to control a weak beam with a strong one.

In this Report, we describe an all-optical switch that combines the extreme sensitivity of instability-generated transverse optical patterns to tiny perturbations (*12*–*16*) with quantum-interference methods (*3*–*10*). A transverse optical pattern is the spatial structure of the electromagnetic field in the plane perpendicular to the propagation direction. As an example, the transverse optical pattern corresponding to two beams of light is a pair of spots. We control such a pattern with a beam whose power is a factor of 6500 times smaller than the power contained in the pattern itself, verifying that the switch is cascadable. Also, the switch is actuated with as few as 2700 photons and thus operates in the low-light-level regime. A measured switching energy density $E \sim 3 \times 10^{-3}$ photons/$(\lambda^2/2\pi)$, where λ = 780 nm is the wavelength of the switching beam, suggests that the switch might operate at the single-photon level with system optimization such as changing the pump-beam size or vapor cell geometry (*17*).

Our experimental setup consists of a weak switching beam that controls the direction of laser beams emerging from a warm laser-pumped rubidium vapor. Two pump laser beams counterpropagate through the vapor and induce an instability that generates new beams of light (i.e., a transverse optical pattern) when the power of the pump beams is above a critical level (*17*), as shown schematically in Fig. 1. The instability arises from mirrorless parametric self-oscillation (*17*–*26*) due to the strong nonlinear coupling between the laser beams and atoms. Mirrorless self-oscillation occurs when the parametric gain due to nonlinear wave-mixing processes becomes infinite. Under this condition, infinitesimal fluctuations in the electromagnetic field strength trigger the generation of new beams of light. The threshold for this instability is lowest (and the parametric gain enhanced) when the frequency of the pump beams is set near the ^{87}Rb $^5S_{1/2} \leftrightarrow {}^5P_{3/2}$ resonance (780-nm transition wavelength). The setup is extremely simple in comparison to most other low-light-level all-optical switching methods (*7*, *8*), and the spectral characteristics of the switching and output light match well with recently demonstrated single-photon sources and storage media (*27*, *28*).

For a perfectly symmetric experimental setup, the instability-generated light (referred to henceforth as "output" light) is emitted both forward and backward along cones centered on the pump beams, as shown in Fig. 1A. The angle between the pump-beam axis and the cone is on the order of ~5 mrad and is determined by competition between two different nonlinear optical processes: backward four-wave mixing in the phase-conjugation geometry and forward four-wave mixing (*17*, *23*, *24*). The generated light has a state of polarization that is linear and orthogonal to that of the linearly copolarized pump beams (*25*); hence, it is easy to separate the output and pump light with the use of polarizing elements. Once separated, the output light propagating in one direction (e.g., the forward direction) can appear as a ring on a measurement screen that is perpendicular to the propagation direction and in the far field (Fig. 1, A and B). This ring is known as a transverse optical pattern (*18*) and is one of many patterns that occur in a wide variety of nonlinear systems spanning the scientific disciplines (*29*).

Weak symmetry breaking caused by slight imperfections in the experimental setup reduces the symmetry of the optical pattern and selects its orientation (*23*). For high pump

Department of Physics, Duke University, Box 90305, Durham, NC 27708, USA.

*To whom correspondence should be addressed. E-mail: gauthier@phy.duke.edu

powers, the pattern consists of six spots with sixfold symmetry, as shown schematically in Fig. 1C. For lower powers near the instability threshold, only two spots appear in the far field in both directions (forward and backward), as shown schematically in Fig. 1D. The azimuthal angle of the spots (and the corresponding beams) is dictated by the system asymmetry, which can be adjusted by slight misalignment of the pump beams or application of a weak magnetic field. The orientation of the spots is stable for several minutes in the absence of a switching beam.

In our all-optical switch, the direction of the bright output beams (total power P_{out}) is controlled by applying a weak switching laser beam with a state of polarization that is linear and orthogonal to that of the pump beams (Fig. 2). The azimuthal angle of the output beams is extremely sensitive to tiny perturbations because the symmetry breaking of our setup is so small (*17*). Directing the switching beam along the conical surface at a different azimuthal angle (Fig. 2B) causes the output beams to rotate to a new angle, while P_{out} remains essentially unchanged. Typically, the orientation of the output beams rotates to the direction of the switching beam and we find that the pattern is most easily perturbed when the switching beam is injected at azimuthal angles of ±60°, thereby preserving the sixfold symmetry of the pattern observed for higher pump powers. Notably, the switching beam also controls the output beams in the backward direction.

We now describe the behavior of our switch for two values of the peak power P_s of the switching beam, where the spots rotate by –60° in the presence of a switching beam. In the absence of a switching beam ($P_s = 0$), we observed the pattern shown in Fig. 3A, where $P_{out} = 1.5$ μW and the total power emitted from the vapor cell in the forward direction in both states of polarization is 19 μW. For the higher power switching beam ($P_s = 2.5$ nW), we observed complete rotation of the output beams (Fig. 3B), whereas we found that only approximately half the power in the beams rotates to the new azimuthal angle (Fig. 3C) at the lower switching power ($P_s = 230$ pW). However, we observed high-contrast switching in both cases.

To quantify the dynamic behavior of the device, we turned the switching beam on and off and measured the resulting change in the output beams. Figure 4, A and B, show the temporal evolution of the power for $P_s = 2.5$ nW on a coarse time, where it is seen that power variation at each location is out of phase, indicating full redirection of the optical power (movie S1).

At higher temporal resolution (Fig. 4C), weak periodic modulation of the emitted light due to a dynamic instability (*25*) is apparent. This modulation corresponds to small fluctuations in the power of the pattern, although its orientation is stable. Even in the presence of this modulation, the contrast-to-noise ratio of the switch is at least 30:1 (defined as the change in power between the on and off states: root-mean-square value of the fluctuations). The rise time of the switch is τ = 4 μs, which we believe is largely governed by the rubidium ground-state optical pumping time (*23*).

Under the conditions shown in Fig. 3B, the total power in the output beams in the forward direction is equal to $P_{out} = 1.5$ μW, whereas the power of the input switching beam is only $P_s = 2.5$ nW. That is, a switching beam controls the behavior of output

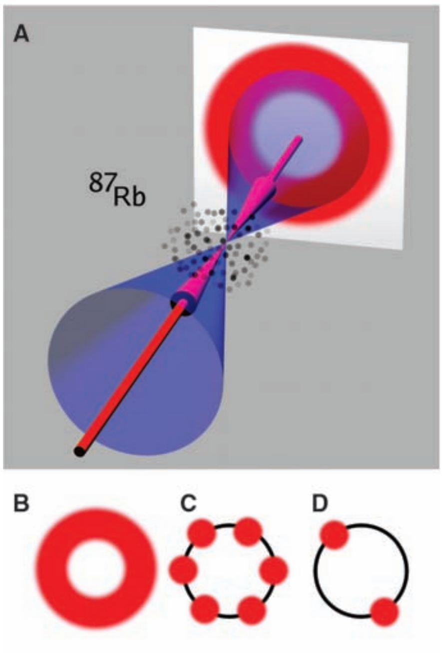

Fig. 1. Generation and symmetry of transverse optical patterns. (**A**) Two linearly copolarized pump beams (red) counterpropagate through warm ^{87}Rb vapor. A modulational instability generates orthogonally polarized light, which is emitted along cones (blue) and forms a transverse optical pattern (red) on a screen perpendicular to the propagation direction. (**B** to **D**) Schematic of the transverse optical pattern for (B) a perfectly symmetric setup, (C) weakly broken symmetry and high pump power, and (D) weakly broken symmetry and low pump power.

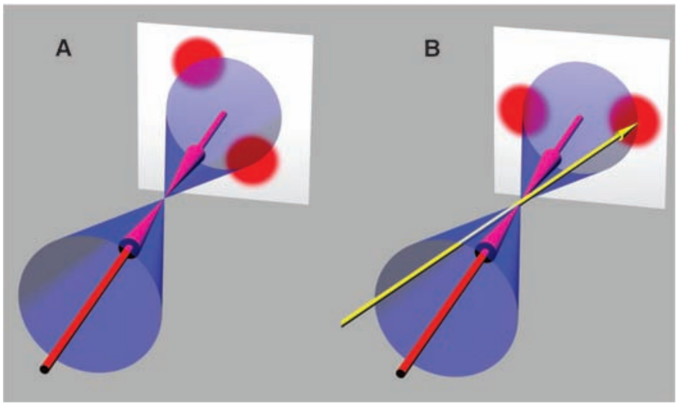

Fig. 2. The two states of the switch. (**A**) The off state. Weak symmetry breaking results in a two-spot output pattern. (**B**) The on state. A weak switching beam (yellow), directed along the cone (blue), causes the output pattern to rotate. The state of polarization of the switching beam (yellow) is linear and orthogonal to that of the pump beams (red).

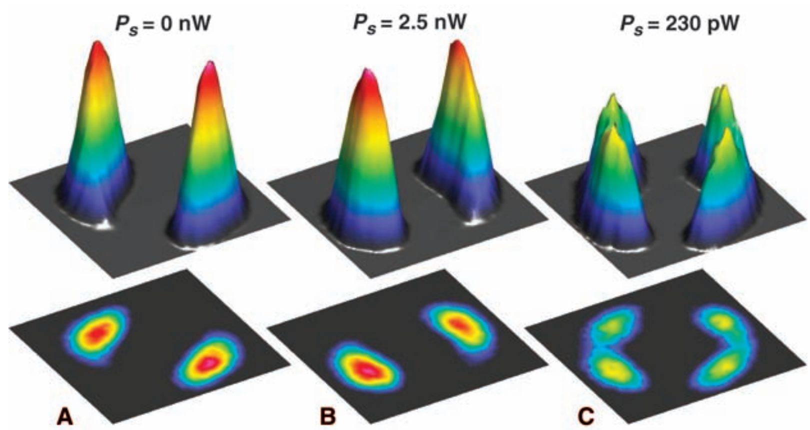

Fig. 3. Low-light-level all-optical switching. The lower panels show a false-color rendition of the detected optical power of the output light (gray, low power; red, high power), and the upper panels are a three-dimensional representation of the same data. (**A**) The off state with $P_s = 0$. The output light forms a two-spot transverse optical pattern. (**B**) The on state with $P_s = 2.5$ nW. The two-spot output pattern is rotated by –60°. (**C**) The on state with $P_s = 230$ pW. Approximately half the output power is rotated by –60°.

beams that are at least 600 times stronger. Based on the time response of the switch, the number of photons needed to change its state is given by $N_p = \tau P_s / E_p = 40{,}000$, where $E_p = 2.55 \times 10^{-19}$ J is the photon energy, and the switching energy is equal to $N_p E_p = 10$ fJ. Optical switches that operate with similarly low energies have been proposed previously, but their application to few-photon switching has not been discussed (*12*, *14*, *15*).

Another metric to characterize low-light-level switches is the energy density E, given in units of photons per $(\lambda^2/2\pi)$. This metric gives the number of photons needed to actuate a switch with a transverse dimension that has been reduced as much as possible—the diffraction limit of the interacting beams (*5*, *11*). For the spot size of the switching beam used in our experiment (1/*e* intensity radius of 166 μm), we find that $E \sim 4.4 \times 10^{-2}$ photons/$(\lambda^2/2\pi)$, corresponding to 11 zeptoJ/$(\lambda^2/2\pi)$.

Similar behavior is observed for the lower switching power, as shown in Fig. 3C. In this case, a weak switching beam controls output beams that are 6500 times stronger. Even though there is only partial switching, the contrast-to-noise ratio is greater than 10:1 (Fig. 4, D and E, and movie S2). As seen in Fig. 4F, $\tau = 3$ μs, which is somewhat faster than that observed at the higher power, possibly due to the fact that only part of the output light rotates to the new angle. Using this response time, we find $N_p = 2700$ photons, $N_p E_p = 690$ aJ, and $E \sim 3 \times 10^{-3}$ photons/$(\lambda^2/2\pi)$ [770 yoctoJ/$(\lambda^2/2\pi)$].

These results demonstrate that a switch based on transverse optical patterns is capable of controlling high-power beams with weak ones, exhibits much higher sensitivity, and can be realized with the use of a simple experimental setup. Such a switch could be used as a binary element in a computation or communication system because, at high switching beam power, our device operates like a transistor used in digital logic (i.e., the transistor's output is either off or saturated). Additionally, this switch could be used as a router if information is impressed on the output light (e.g., by modulating the pump beams).

For comparison, the sensitivity of our switch, characterized by E, far exceeds that demonstrated by other methods such as electromagnetically induced transparency (EIT). To date, the best EIT-based switch results have been reported by Braje *et al*. (*8*) who have achieved $E \sim 23$ photons/$(\lambda^2/2\pi)$; our switch is more than 5000 times as sensitive. Furthermore, the EIT experimental setup is much more complicated, requiring the use of cooled and trapped rubidium atoms and limited to output beams that are much weaker than the input switching beam. Recently, a transient switch based on laser beams propagating through a warm rubidium vapor in a simple setup has been reported, but it does not operate in the low-light-level regime (*10*).

Although speculative, our technique might be useful at telecommunication wavelengths where high-quantum efficiency, low-noise, single-photon detectors are difficult to realize. For these wavelengths, the rubidium vapor could be replaced with a molecular gas, such as acetylene or hydrogen cyanide, both of which have resonances in the telecommunications band. A low-light-level incident beam could then be detected by switching the output beam onto a standard telecommunications-band detector.

In addition, our general method of exploiting the sensitivity of patterns to small perturbations may find application in other scientific disciplines. For example, modulational instabilities, which often give rise to pattern formation, have been observed in matter waves created with ultracold quantum gases (*30*), suggesting that atom switching might be possible by perturbing the gas with a few injected atoms.

Our results may also have implications concerning the fundamental limits of general-purpose computation devices. Many years ago, Keyes (*11*) realized that thermal energy dissipation places limits on the operational speed of a logic element. By assuming that a saturation-based optical switch has $E \sim 1$ photon/$(\lambda^2/2\pi)$, he concluded that optical logic elements are limited to rates below 10^{10} s^{-1}. Our observed switching energy density is more than a factor of 300 below that assumed by Keyes, suggesting that optical devices might surpass his estimated limit.

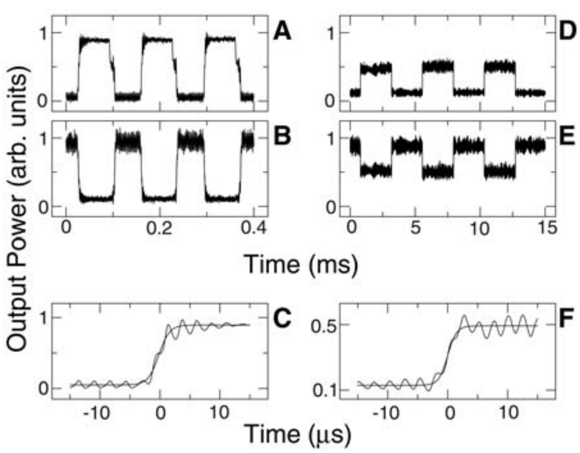

Fig. 4. Dynamical behavior of the low-level all-optical switch. In the plane of the measurement screen, we place one aperture at the center of one of the spots shown in Fig. 3A (the off state of the switch) and another at the center of one of the spots shown in Fig. 3B (the on state). Temporal evolution of the output power passing through (**A** and **C**) the on-state aperture for P_s = 2.5 nW, (**B**) the off-state aperture for P_s = 2.5 nW, (**D** and **F**) the on-state aperture for P_s = 230 pW, and (**E**) the off-state aperture for P_s = 230 pW. The fit lines in (C) and (F) are determined using a sigmoidal function. The rise-time of the switch based on this fit is (C) τ = 4 μs for P_s = 2.5 nW and (F) τ = 3 μs for P_s = 230 pW. arb. units, arbitrary units.

References and Notes

1. R. Ramaswami, K. N. Sivarajan, in *Optical Networks: A Practical Perspective* (Morgan Kaufmann, San Francisco, CA, ed. 2, 2002), ch. 12.
2. H. M. Gibbs, *Optical Bistability: Controlling Light with Light* (Academic Press, Orlando, FL, 1985).
3. M. D. Lukin, *Rev. Mod. Phys.* **75**, 457 (2003).
4. H. Schmidt, A. Imamoglu, *Opt. Lett.* **21**, 1936 (1996).
5. S. E. Harris, Y. Yamamoto, *Phys. Rev. Lett.* **81**, 3611 (1998).
6. M. D. Lukin, A. Imamoglu, *Phys. Rev. Lett.* **84**, 1419 (2000).
7. M. Yan, E. G. Rickey, Y. Zhu, *Phys. Rev. A.* **64**, 041801 (2001).
8. D. A. Braje, V. Balić, G. Y. Yin, S. E. Harris, *Phys. Rev. A.* **68**, 041801 (2003).
9. K. J. Resch, J. S. Lundeen, A. M. Steinberg, *Phys. Rev. Lett.* **89**, 037904 (2002).
10. I. Novikova, A. S. Zibrov, D. F. Phillips, A. André, R. L. Walsworth, *Phys. Rev. A.* **69**, 061802 (2004).
11. R. W. Keyes, *Science* **168**, 796 (1970).
12. C. P. Smith *et al.*, *Opt. Commun.* **102**, 505 (1993).
13. R. Martin, A. J. Scroggie, G.-L. Oppo, W. J. Firth, *Phys. Rev. Lett.* **77**, 4007 (1996).
14. F. Prati, M. Travagnin, L. A. Lugiato, *Phys. Rev. A.* **55**, 690 (1997).
15. S. Barland *et al.*, *Nature* **419**, 699 (2002).
16. B. Gütlich, R. Neubecker, M. Kreuzer, T. Tschudi, *Chaos* **13**, 239 (2003).
17. Materials and methods are available as supporting material on *Science* Online.
18. L. A. Lugiato, *Chaos Solitons Fractals* **4**, 1251 (1994).
19. S. E. Harris, *Appl. Phys. Lett.* **9**, 114 (1966).
20. A. Yariv, D. M. Pepper, *Opt. Lett.* **1**, 16 (1977).
21. Y. Silberberg, I. Bar-Joseph, *J. Opt. Soc. Am. B* **1**, 662 (1984).
22. G. Khitrova, J. F. Valley, H. M. Gibbs, *Phys. Rev. Lett.* **60**, 1126 (1988).
23. A. Maître, A. Petrossian, A. Blouin, M. Pinard, G. Grynberg, *Opt. Commun.* **116**, 153 (1995).
24. W. J. Firth, A. Fitzgerald, C. Paré, *J. Opt. Soc. Am. B* **7**, 1087 (1990).
25. D. J. Gauthier, M. S. Malcuit, A. L. Gaeta, R. W. Boyd, *Phys. Rev. Lett.* **64**, 1721 (1990).
26. S. Zibrov, M. D. Lukin, M. O. Scully, *Phys. Rev. Lett.* **83**, 4049 (1999).
27. C. H. van der Wal *et al.*, *Science* **301**, 196 (2003).
28. J. McKeever *et al.*, *Science* **303**, 1992 (2004).
29. M. C. Cross, P. C. Hohenberg, *Rev. Mod. Phys.* **65**, 851 (1993).
30. K. E. Strecker, G. B. Partridge, A. G. Truscott, R. G. Hulet, *Nature* **417**, 150 (2002).

31. We thank K. Gibble for discussions of rubidium cells and the DARPA DSO Slow-Light Program, NSF, and the U.S. Army Research Office for financial support.

Supporting Online Material
www.sciencemag.org/cgi/content/full/308/5722/672/DC1
Materials and Methods
Figs. S1 and S2
Movies S1 and S2

24 January 2005; accepted 11 March 2005
10.1126/science.1110151